PORT SAID ENGINEERING RESEARCH JOURNAL
Faculty of Engineering - Port Said University
Volume 29, No. 3 pp:52:62

Behavior of Confined Concrete Filled FRP Tube Under Lateral Loads

Mohamed Hamed [1], Ibrahim El Arabi [2], Ahmed Elbarbary [3], Mahmoud El Gendy [4]*

[1]*Assistant Prof., Civil Engineering Department, Faculty of Engineering, Port Said University,*
E-mail: mohamed.hamed@eng.psu.edu.eg
[2]*Associate Prof., Faculty of Engineering, Delta University for Science and Technology,*
E-mail: ibrahim.alaraby@deltauniv.edu.eg
[3]*Master Student, Civil Engineering Department, Faculty of Engineering, Port Said University,*
E-mail: ahmed.hesham@eng.psu.edu.eg, https://orcid.org/0009-0002-3354-4859
[4]*Assistant Prof., Civil Engineering Department, Faculty of Engineering, Port Said University,*
E-mail: mahmoud.mohamed@eng.psu.edu.eg, http://orcid.org/0000-0003-2696-7917

**Corresponding author*: ahmed.hesham@eng.psu.edu.eg, *DOI: 10.21608/pserj.2025.373479.1403*

Received 7-4-2025,
Revised 6-5-2025,
Accepted 19-5- 2025

ABSTRACT

This paper presents the application of advanced numerical modeling in geotechnical engineering for analyzing the lateral load response of confined concrete-filled fiber-reinforced polymer (*FRP*) tube piles, addressing the growing need for innovative foundation solutions in challenging soil conditions. Extending the authors' previous investigations into laterally loaded piles and confined concrete-filled *FRP* tubes, the developed numerical approach, a hybrid technique implemented in *GEOTools* software, utilizes the *P-y* curve method to model nonlinear soil behavior and incorporates nonlinear material properties derived from the stress-strain characteristics of the FRP tube and confined concrete. The technique was used to investigate the influence of key material and geometric parameters, including concrete compressive strength and diameter-to-thickness ratios, on the pile's load capacity, deformation, and stability. The numerical framework's accuracy is validated against interaction diagrams from international design codes, experimental data, and analytical results from the literature. Furthermore, a practical application is demonstrated by modeling FRP piles in a realistic East Port Said subsoil profile. Results show a strong correlation between pile geometric ratios and lateral performance. Maximum bending moment and shear force were found to be influenced by the length-to-diameter ratio up to 15, beyond which further increases had no impact as the pile reached its effective length. Additionally, increasing the diameter-to-FRP thickness ratio enhanced moment and shear resistance.

Keywords: Laterally loaded piles, *FRP* Piles, Concrete-Filled *FRP*, Deep foundations, East Port Said.

1. INTRODUCTION

Concrete-filled *CFRP* tubes, eliminating the need for steel reinforcement, provide a high-strength composite pile system, particularly advantageous in marine environments due to their corrosion resistance. The lateral confinement provided by the *CFRP* tube enhances the concrete's structural capacity, improving axial and lateral load-bearing capabilities. Performance is contingent on several design parameters, including concrete core strength, *CFRP* material characteristics, tube thickness, and the length-to-diameter (*L*/*D*) ratio. Optimization of these factors is critical to maximizing structural efficiency. The inherent durability, reduced maintenance, lightweight nature, and ease of installation of *CFRP* tube piles contribute to their growing adoption as a viable alternative to traditional piling methods.

Several studies have extensively investigated the structural behavior of fiber-reinforced polymer (*FRP*) and composite piles under various loading conditions, providing valuable insights into their performance and effectiveness in different environments. *Zhang et al.* [34] examined two strengthening techniques for concrete-filled steel tubes (*CFST*) under axial loads, namely *FRP* wrapping and welded steel strips, revealing that both methods significantly enhanced load-bearing capacity and deformation resistance, especially with increased material thickness. While welded steel strips were 40% more cost-effective, *FRP* demonstrated superior durability in harsh environments, particularly marine conditions. Similarly, *Malik et al.* [23] explored the

behavior of *FRP*-reinforced seawater sea-sand concrete (*SSC*) composite piles under static loading. Their findings showed strain concentrations near the pile head, leading to failure, with maximum shaft friction mobilization in the upper third of the socket.

Al-Darraji et al. [2] studied confined concrete-filled aluminum tube (*CCFAT*) piles under combined vertical and lateral loads, demonstrating that vertical load capacity increased with slenderness ratio (*Lm/d*), while lateral capacity improved with higher vertical loads. The study identified shear failure as the dominant failure mechanism and highlighted the significant influence of internal friction angle and Young's modulus on pile behavior. Also, *Otoom et al.* [25] investigated *GFRP* confinement effects on different infill materials such as concrete, grout, and epoxy, concluding that *GFRP* wrapping significantly improved compressive strength and modulus of elasticity, with a strong correlation between experimental and numerical results, reinforcing its effectiveness in structural retrofitting.

Dhatrak et al. [5] performed numerical analysis of an *FRP* pile model using *MIDAS GTS NX* software to analyze various parameters such as slenderness ratio, *FRP* thickness, pile group configurations, and material types under vertical and lateral loads. Their study showed that single *FRP* piles had greater load-bearing capacity than conventional concrete piles, with *CFRP* outperforming GFRP in terms of ultimate capacity, and the optimal *L/D* ratio determined to be equals to 45. Furthermore, *Pando et al.* [26] investigated the long-term durability of concrete-filled FRP tube (*CCFT*) piles, finding that submergence time and moisture content significantly influenced strength, with *FRP* shell degradation reducing flexural strength by 20% over time. In addition, *Kim et al.* [20] studied fiber-reinforced plastic helical screw piles, reporting a close match between predicted and actual failure strengths, with minimal error. Also, *Lee et al*. [22] further demonstrated that composite concrete piles (*CCFT*) exhibited higher strength than plain concrete piles and standalone *FRP* tubes due to confinement effects, with increased slenderness ratio leading to reduced strength and ductility. *Kim* [21] examined FRP-concrete composite piles incorporating modular pultruded *FRP* (*PFRP*) members, identifying significant discrepancies between flexural test results and predictive formulas, highlighting the need for improved design methodologies. Collectively, these studies provide crucial insights into the structural behavior, durability, and optimization of *FRP* and composite pile systems, emphasizing their advantages in enhancing load capacity, energy absorption, and long-term stability, particularly in marine and seismic applications. They also underscore the importance of parameters such as slenderness ratio, infill material properties, impact resistance, and confinement techniques in determining overall structural performance.

In this study, the *GEOTools* program, a component of the *ELPLA* software (*El Gendy et al.* [7]), is utilized for analyzing piles and geotechnical structures. Originally developed for single piles, pile groups, and piled rafts under vertical loads, *ELPLA* employs both the Winkler model, and a continuum approach based on Mindlin equations (*El Gendy et al.* [8], [12]). A nonlinear analysis capability, built on a hyperbolic function by *Russo* [30], has been incorporated and applied in several studies (*El Gendy et al.* [10], *El Kamash et al.* [17], *Ibrahim et al.* [19], and *Mohamedien et al.* [24]). The program has been further enhanced to estimate piled raft settlements using vertical load tests, including applications in Burj Khalifa's foundation analysis (*El Gendy et al.* [11]). The Mindlin-based hyperbolic model was extended to analyze laterally loaded piles of circular and rectangular cross-sections (*El Gendy et al.* [13], [14[, [15], [16], *Ghatass et al.* [18]).

A numerical technique for analyzing laterally loaded piles and confined concrete-filled *FRP* tubes, previously presented by the authors [6], [9], is extended in this study to investigate the influence of key material and geometric parameters, including concrete compressive strength and diameter-to-thickness ratios, on the pile's load capacity, deformation, and stability. The approach models the pile as a nonlinear beam on a Winkler foundation, employing 1*D* finite elements with bending stiffness governed by various design codes (*ACI*318, *EC*2, *ECP*, *BS*8110, etc.). Soil deformation is evaluated using P-y curves derived from full-scale field tests across 14 soil models. The analysis incorporates Euler and Timoshenko beam theories and optimizes computational efficiency by reducing the number of equations. Unlike some common software such as *SPColumn* [33], *Lpile* [27], *Pypile* [35], and *RSPile* [31], which rely primarily on *ACI*318 [1], GEOTools was validated through comprehensive comparative studies comparing its results with experimental data and numerical results obtained using different available software.

This study aims to investigate the impact of material and geometric parameters on the lateral load capacity of fiber-reinforced polymer (*FRP*) tube piles filled with concrete, with a focus on identifying the most influential factors and key dimensional ratios such as pile diameter, diameter-to-thickness (*D/t*), and length-to-diameter (*L/D*) ratios. Correlation analysis is conducted to assess the relationships between these parameters and their effects on maximum bending moment and shear forces. The research also addresses a gap in international design codes regarding permissible lateral displacement limits for piles, noting that only the International Building Code (*IBC*) and the Indian Standard provide explicit criteria. Displacement limits from these codes were adopted to standardize the evaluation process and analyze the influence of different parameters under consistent conditions. The analysis was performed using *GEOTools* software, whose accuracy was verified through comparisons with analytical results from the literature and outputs from alternative established software. A comprehensive parametric study was carried

out considering real subsoil conditions, using the soil properties and stratification of East Port Said as a case study to examine the effects of pile dimensions and material properties on lateral performance. The findings offer practical guidelines for the analysis and design of laterally loaded FRP piles, applicable to East Port Said and similar soil formations worldwide.

2. VALIDATION

The developed program, GEOTools [7], was validated by comparing the interaction diagrams generated from analyzing circular columns with the available interaction diagram in the ECP [4]. Additionally, Lpile [27] and GEOTools software were used to simulate the behavior of circular concrete-filled fiber-reinforced polymer (FRP) columns, and the results were compared with experimental data reported by Rocca et al. [28]. Furthermore, Lpile [27] and GEOTools [7] software were used to simulate the behavior of a laterally loaded concrete-filled steel tube (CFST) pile, comparing the results with those obtained experimentally by Rollins et al. [29]. The soil conditions were complex, consisting of multiple clay and sand layers.

2.1. Comparative study between *GEOTools* and the Egyptian code

A verification example of a circular reinforced concrete section is presented. This circular column exhibits a cross-sectional diameter of 800 mm. The concrete's compressive strength fcu is 25 MPa, while the steel's modulus of elasticity Es is 200 GPa. Additionally, the steel's ultimate strength fy is 400 MPa. 32 bars, each possessing a bar diameter of 32 mm. The clear cover to the edge of the longitudinal bar measures 30 mm. Results from GEOTools selecting the ECP design code in the analysis were compared with the available interaction diagram in the Egyptian code (ECP) [4] as shown in in Figure 1:. This figure shows the relationship between axial load and bending moment capacity, demonstrating the accuracy of GEOTools in predicting column behavior according to the ECP code, and highlighting the impact of safety factors by showing a lower capacity for the factored results compared to the nominal results.

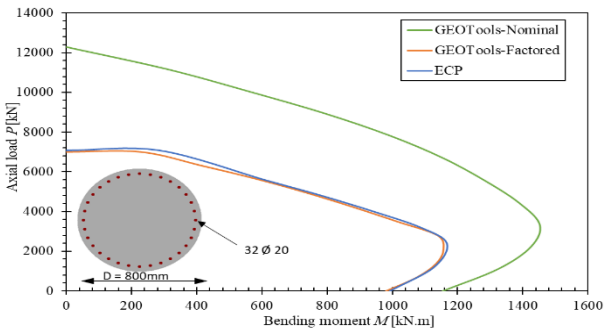

Figure 1:Comparison between interaction diagram using ECP code by *GEOTools* and the design aids for the Egyptian code

2.2. Comparative study between *GEOTools*, *Lpile*, and literature results

Rocca et al. [28] investigated the interaction diagram method for FRP-confined concrete columns with both circular and non-circular sections. The columns were constructed from concrete-filled FRP tubes with longitudinal steel reinforcement bars. This study focuses on the results obtained for columns with circular sections. Their investigation considered the key characteristics of FRP, reinforcing steel (RFT), and concrete, as outlined by the ACI code. Three specimens with varying properties were analyzed, including specimen diameter D (mm), height H (m), concrete compressive strength f'c (MPa), yield stress of steel fy (MPa), longitudinal steel reinforcement ratio ρ (%), FRP modulus of elasticity Ef (GPa), FRP ultimate tensile strength ffu (MPa), tube thickness tf (mm), as listed in Table 1.

Table 1. Properties of the concrete, *RFT* steel and *FRP* materials, *Rocca et al.* [28]

No.	D mm	H m	f'_c MPa	f_y MPa	ρ %	E_f GPa	f_{fu} MPa	t_f mm
1	305	1.62	38.3	358	2.47	18600	532	0.8
2	356	1.47	40.4	500	3.01	20800	416	1.25
3	508	1.73	38	400	1.78	60000	700	0.9

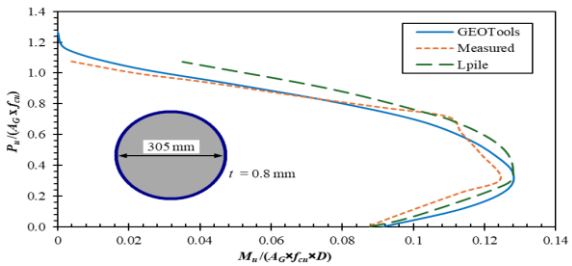

Figure 2:Interaction diagram of Specimen No. 1

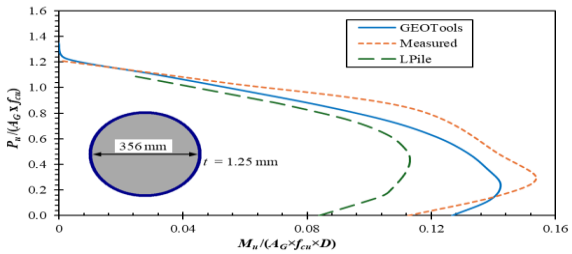

Figure 3:Interaction diagram of Specimen No. 2

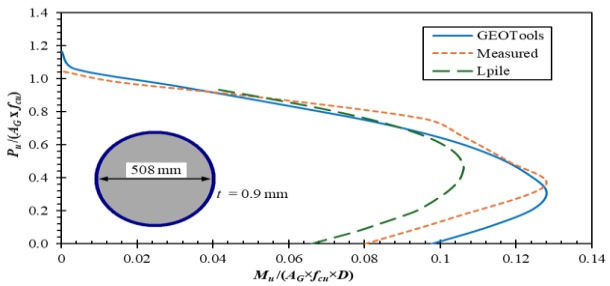

Figure 4:Interaction diagram of Specimen No. 3

The experimental data from Table 1 served as input parameters for modeling the test specimens using both LPile and GEOTools software. The validation process involved generating and comparing interaction diagrams for multiple composite section samples. Figure 2: through Figure 4: present the numerical analysis results alongside the corresponding field measurements for the three samples.

Figure 2: shows that the GEOTools results in a compression failure zone that more closely matches the measured data, with a mean absolute percentage error (MAPE) of 1.52% compared with the LPile's MAPE of 2.43%. Conversely, in the tension failure zone, the LPile results are slightly closer to the measured data, with a MAPE of 3.17%, although the difference between the two software programs is minimal. As shown in Figure 3:, the LPile results deviate in both the compression and tension zones, with a MAPE of 15%. The GEOTools results are significantly more accurate in these zones, with a MAPE of 6.02%. Figure 4: is similar to Figure 3:, the LPile results diverge in both the compression and tension zones, with a MAPE of 10.40%. The GEOTools provides results that substantially better align with the measured data in these areas, with a MAPE of 6.55%. Overall, both the LPile and GEOTools programs demonstrated a high level of agreement between the experimental and computed values for the three samples.

2.3. Case study of laterally loaded pile

Rollins et al. [29] numerically studied a group of piles under lateral loads and compared their behavior with that of a single pile. These piles consisted of concrete-filled steel tubes CFST. The group consisted of piles with a 0.305 m internal diameter and a wall thickness of 9.5 mm. The pile length was approximately 11 m. The modulus of elasticity of the concrete was 17.5 GPa, and its strength was 20.7 MPa. The load was applied at a point 0.4 m above ground level.

Table 2. Values of the soil properties at the Salt Lake International Airport, *Rollins et al.* [29]

Z (m)		Soil	$C_u - \varphi$	γ
From	to	Type	(kN/m^2- °)	(kN/m^3)
0.4	0.87	Clay	46 - 0	8.186
0.87	1.12	Clay	41.6 - 0	8.828
1.12	1.50	Clay	59 - 0	8.828
1.50	2.27	Clay	50 - 0	8.828
2.27	3.27	Clay	41 - 0	9.671
3.27	5.07	Clay	38 - 0	10.055
5.07	5.47	Clay	52.3 - 0	6.302
5.47	6.07	Clay	25 - 0	10.055
6.07	6.77	Clay	51 - 0	10.055
6.77	9.77	Sand	0 - 36	9.315

The ground beneath the piles at the Salt Lake International Airport consists of soft to medium clay layers on top of alternating layers of sand and finer soils. Details about these layers, obtained from field and laboratory tests, are provided in Table 2. Each layer is characterized by specific properties: the depth from the ground surface (Z), unit weight (γ), angle of internal friction of the sand (φ), and the undrained shear strength of the soil (Cu).

This case uses a hybrid computational approach to analyze the behavior of nonlinear laterally loaded concrete–filled steel piles embedded in multilayered soil. The method considers the nonlinearity of the pile material. The results obtained via the LPile and GEOTool programs, including pile head displacements and bending stiffnesses against moments, are compared with those of available field measurements conducted by Rollins et al. [29] to ensure the accuracy and reliability of the computational models. Figure 5: shows the comparison of the relationships between the bending stiffness EI and the bending moment M with mean absolute percentage errors (MAPEs) of 3.6% and 10.2% for both the LPile and GEOTool programs, respectively, whereas Figure 6: compares the computed and measured results of the pile head displacements with MAPEs of 5.65% and 3.40% for both the LPile and GEOTool programs, respectively. Overall, the experimental and computed values for the test conducted at Salt Lake showed an extremely high level of agreement when both the LPile and GEOTool programs were used.

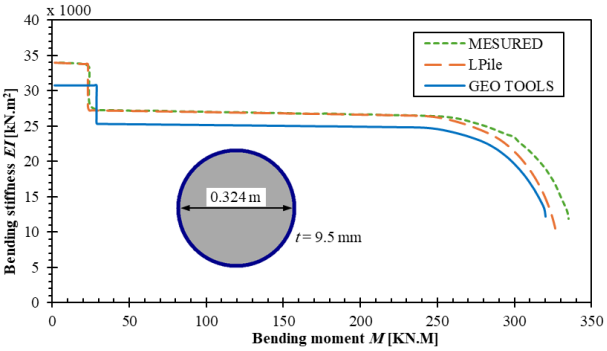

Figure 5:Relation between the bending stiffness *EI* and the bending moment *M*

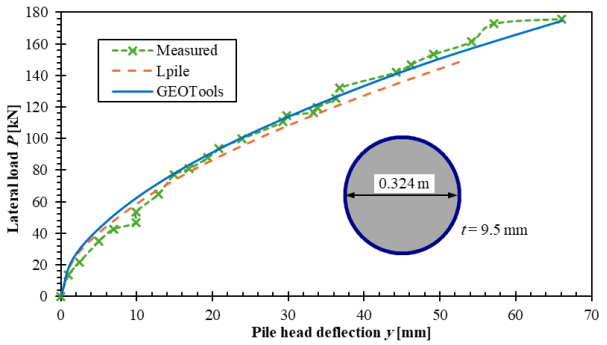

Figure 6:Relationships between load and pile head displacement

3. PARAMETRIC STUDY

This section details a parametric study investigating the behavior of laterally loaded FRP piles embedded in the specific subsoil conditions of East Port Said. The study aims to analyze the impact of material and geometric parameters on the lateral load capacity of fiber-reinforced polymer (FRP) tube piles filled with concrete, focusing on factors such as diameter-to-thickness (D/t) and length-to-diameter (L/D) ratios in this region. The necessity for this analysis arises from the prevalent soft clay layers, which pose significant soil challenges for structures in East Port Said, similar to those encountered in locations like London, Frankfurt, Rome, and Dammam.

The analysis incorporates typical subsoil layers found in East Port Said, based on data from various soil investigation reports (Table 3). This subsoil model consists of seven distinct layers, each characterized by specific properties: the depth from the ground surface (Z), unit weight (γ), shear strength parameters (c, φ), undrained shear strength (cu), and strain corresponding to half of the maximum principal stress difference (ε50). And the stable ground water table was observed at the time of investigation at depth of (-1 m) from the ground surface.

Table 3. Soil properties of the East Port Said region

Z (m)	Description	φ (°)	*c* (KPa)	C_U (KPa)	γ (kN/m³)	ε50
0	Fill	-	-	-	-	-
3.3	Soft silty clays, sandy silts and silty fine sands.	30	20	36	17.8	0.002
9.9	Medium dense to dense silty fine sand with traces of shell.	32	0	0	16.3	0.005
14.5	Sily clay, sandy silt and silty fine sand.	12.5	28.5	30.7	16.8	0.003
25	Thick soft high plasticity clay	0	15	21.4	14.5	0.002
47.7	Thick medium stiff high plasticity clay with increasing strength with depth.	0	39.3	56.1	17.9	0.002
60	Dense to very dense, fine to medium sand.	40	0	0	18	0.005

This study utilizes GEOTools software, employing nonlinear stiffness values derived from ECP [4] building codes. Soil deformation is modeled using P-y curves, which are based on full-scale field tests for various soil types. A parametric analysis was performed, exploring different FRP pile designs by varying FRP tube thickness (t), pile diameter (D), pile length (L), and concrete strength (fcu) (Table 4). The FRP material properties, modulus of elasticity (Ef) and ultimate strength (ffu), were held constant at 152 GPa and 500 MPa, respectively.

Table 4. The range of variable parameters and their intervals

Parameters	From	To	Int.
Tube thickness *t* (mm)	6	14	2
Diameter *D* (m)	0.4	1.2	0.2
Pile Length *L* (m)	4	36	4
Concrete strength f_{cu} (MPa)	25	50	5

Pile capacity was determined at the maximum allowable lateral displacement of 2.5 cm, as specified by the International Building Code [3] and SNI 8460-2017 [31]. The study investigated pile capacity and the impact of various parameters at this displacement limit.

3.1. Effect of *L/D* ratio on capacity of *FRP* pile.

The study examined the effect of the length-to-diameter (L/D) ratio on lateral displacement, shear, and moment diagrams. For a concrete strength of 30 MPa, L/D ratios of 5, 10, 15, 20, 25, 30, 35, 40, and 45 were investigated, using the real soil properties listed in Table 3. Pile capacity was assessed at a maximum lateral displacement of 2.5 cm.

The analysis presented in Figure 7: through Figure 11: shows distinct stages of pile behavior based on the L/D ratio and the normalized vertical depth from the ground surface Z/L. Initially, the increasing L/D increases maximum moment and shear. Once L/D reaches 15, these values plateau, signifying the effective length. Below this, at L/D = 5, the pile behaves rigidly, and at L/D = 10, it exhibits semi-elasticity. Beyond L/D = 15, the pile reaches its maximum capacity, and further length increases have no impact on displacement, shear, or moment.

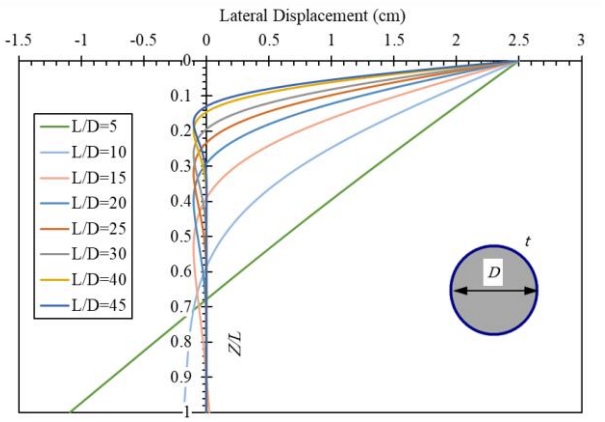

Figure 7: The relation between *Z/L* and lateral displacement for different *L/D*

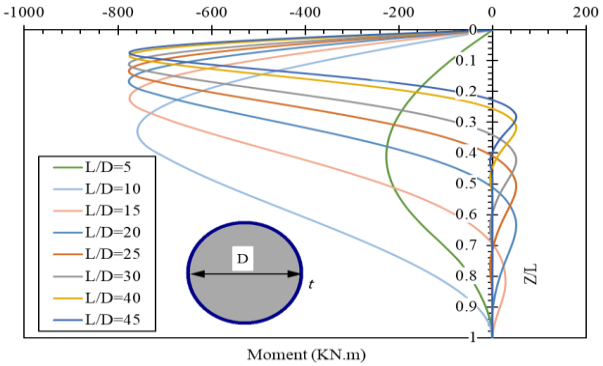

Figure 8:The relation between *Z/L* and moment at displacement =2.5 (cm)

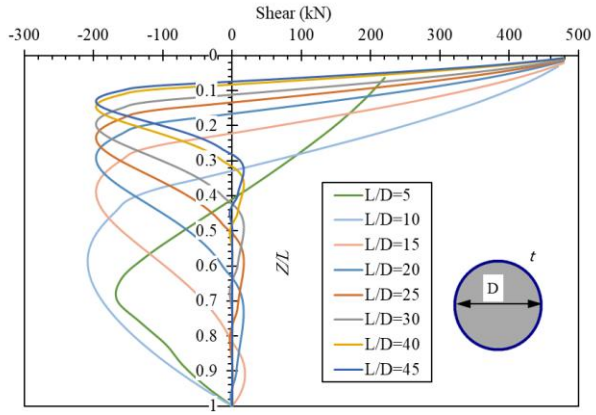

Figure 9:The relation between *Z/L* and Shear at displacement =2.5 (cm)

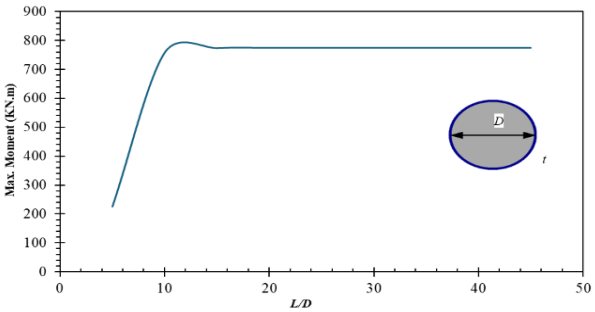

Figure 10:The relation between Max. Moment and *L/D*

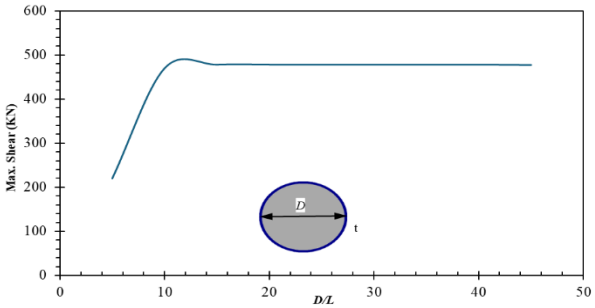

Figure 11:The relation between Max. Shear and *L/D*

3.2. Effect of *D/t* ratio on capacity of *FRP* pile.

This study analyzed the impact of the diameter-to-thickness (D/t) ratio on lateral displacement, shear, and moment diagrams. Two scenarios were examined: first, a constant diameter (D = 80 cm) with varying tube thickness (t), and second, a fixed tube thickness (t = 10 mm) with a variable diameter (D). A 24-meter-long pile with a concrete strength of 30 MPa was utilized. Normalized lateral displacement, shear force, and moment curves were evaluated using the real soil properties listed in Table 3. Pile capacity was assessed based on a maximum allowable lateral displacement of 2.5 cm.

3.2.1. Case (1): Constant diameter

In this scenario, the D/t ratio varied from 57 to 130, while the L/D ratio remained constant at 30. A constant diameter of 80 cm was maintained for a 24 m long pile with a concrete strength of 30 MPa. The normalized displacement, moment, and shear values are depicted in Figure 12: through Figure 16:. As observed, the pile's capacity to resist moment and shear forces increases as the D/t ratio decreases. Consequently, this highlights the significant impact of increasing tube thickness on the pile's capacity when the diameter is held constantly.

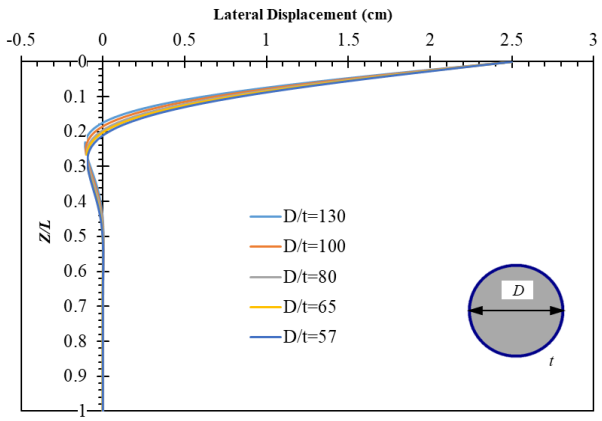

Figure 12:The relation between *Z/L* and lateral displacement

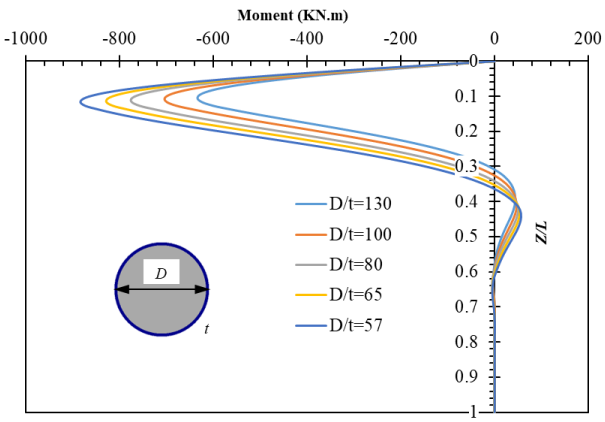

Figure 13:The relation between *Z/L* and moment at displacement =2.5 (cm)

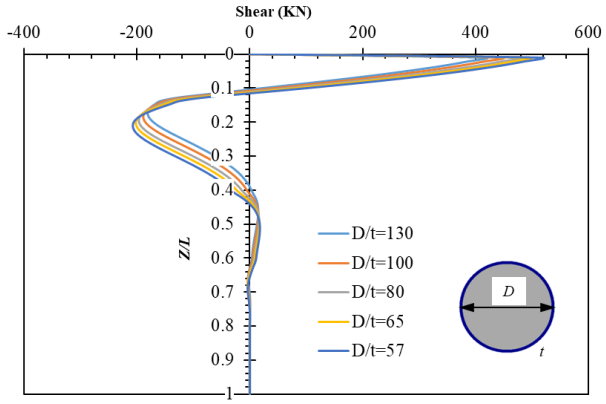

Figure 14:The relation between *Z/L* and Shear at displacement = 2.5 (cm)

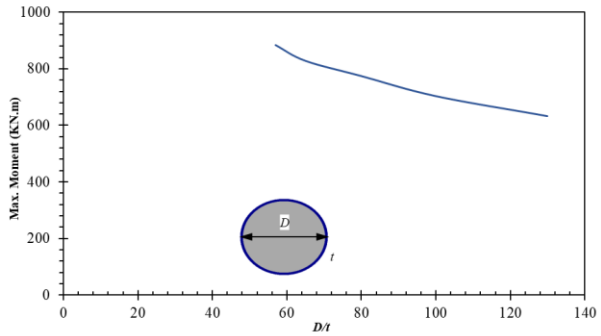

Figure 15:The relation between Max. moment and *D/t*

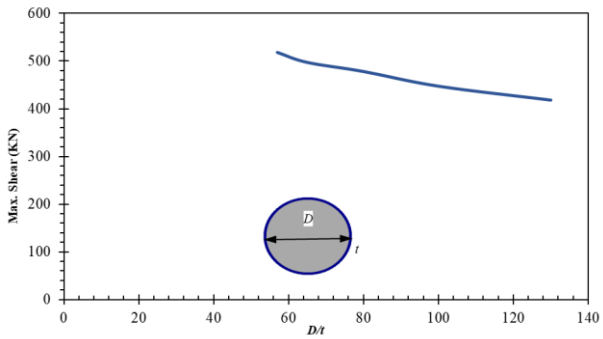

Figure 16:The relation between Max. Shear and *D/t*

3.2.2. Case (2) Constant tube thickness

In this scenario, the D/t ratio varied from 40 to 120, while the tube thickness remained constant at 10 mm for a 24-meter-long pile with a concrete strength of 30 MPa. This resulted in a variable L/D ratio (20, 24, 30, 40, and 60), all exceeding 15, indicating that the length had no effect as the pile reached its effective length, as presented in section 3.1.

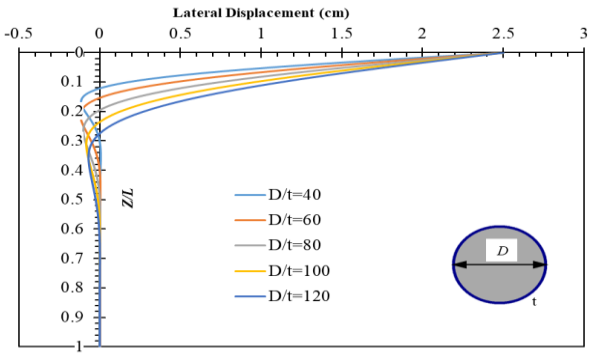

Figure 17:The relation between *Z/L* and lateral displacement

The normalized displacement, moment, and shear values are depicted in Figure 17: through Figure 21:. The results indicate that as the D/t ratio increases, the pile's capacity to resist both moment and shear forces also increases. This highlights the critical role of pile diameter in enhancing load-bearing performance. With a constant tube thickness, the increase in diameter directly contributes to improved structural strength, suggesting that larger diameters facilitate better load distribution and higher resistance. Therefore, the influence of pile diameter is more pronounced when the thickness is fixed.

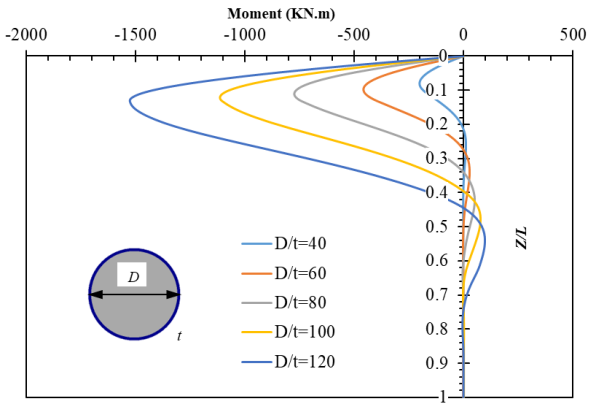

Figure 18:The relation between *Z/L* and moment at displacement =2.5 (cm)

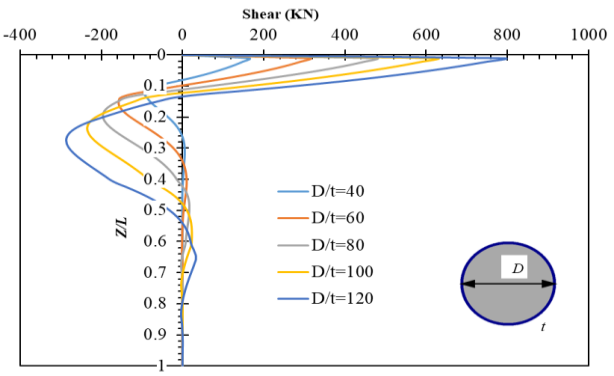

Figure 19:The relation between *Z/L* and Shear at displacement =2.5 (cm)

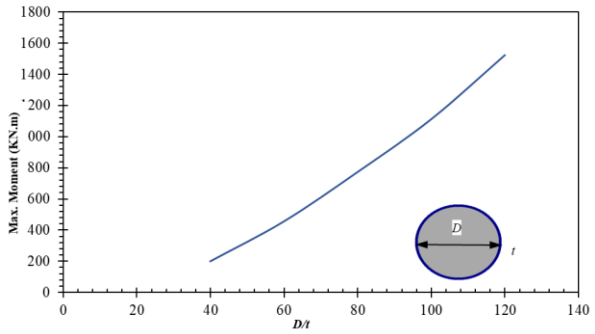

Figure 20:The relation between Max. moment and *D/t*

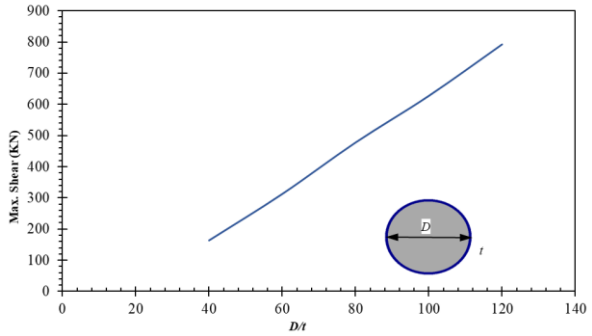

Figure 21:The relation between Max. Shear and *D/t*

3.3. Effect of concrete strength on the capacity of pile/column according to *EPC.*

The impact of concrete strength on FRP tube pile behavior was investigated using displacement, moment, and shear diagrams. Analyses were performed for concrete strengths ranging from 25 to 50 MPa, in accordance with EPC standards. The D/t ratio was 80, and the L/D ratio was 30.

As illustrated in Figure 22: through Figure 24:, the effect of concrete strength on the pile's load-bearing capacity under lateral loads is not significant. The changes in lateral displacement, moment, and shear are minimal, exhibiting almost negligible differences. This suggests that variations in concrete strength have little influence on the pile's overall structural behavior when subjected to lateral forces. While concrete strength is a critical factor in many load-bearing scenarios, its impact under lateral loading conditions appears to be minor. Consequently, the pile's resistance to lateral loads remains relatively consistent, even with small changes in concrete strength. This is likely due to soil failure occurring before material failure.

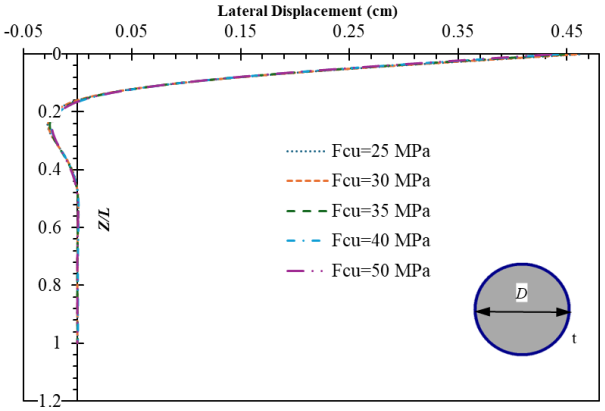

Figure 22:The relation between *Z/L* and displacement

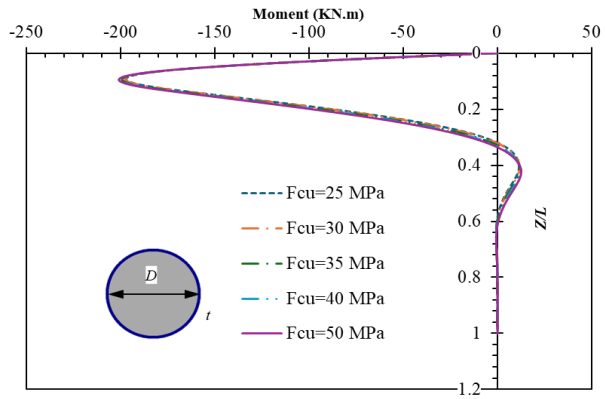

Figure 23:The relation between *Z/L* and Moment

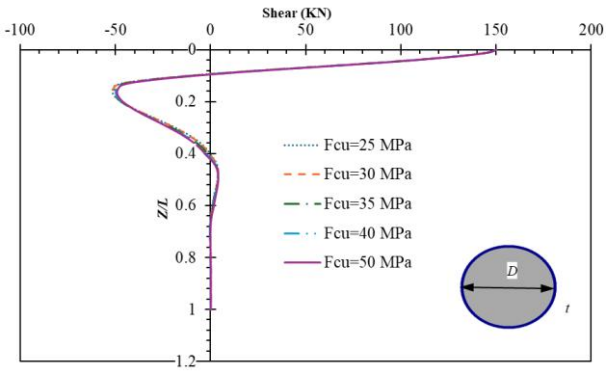

Figure 24:The relation between *Z/L* and Shear

4. CORRELATION ANALYSIS

A correlation matrix is commonly used to visualize these relationships, often represented as a heatmap where color intensity indicates the strength of correlation. In this approach, a positive correlation suggests that an increase in one variable leads to an increase in another, while a negative correlation implies an inverse relationship. If the correlation coefficient is close to 1 or -1, the relationship is strong, whereas values near 0 indicate weak or negligible correlation. Noting that Correlation only measures linear relationships. It's possible that non-linear relationships exist between these

variables, which wouldn't be captured by the correlation coefficient.

In structural applications, correlation analysis is particularly valuable in studying the relationships between geometric properties (such as length, diameter, and thickness) and mechanical performance indicators (such as maximum moment and shear force). Understanding these correlations helps engineers make informed decisions regarding material proportions, load distribution, and failure mechanisms, ultimately contributing to safer and more efficient structural designs.

Figure 25: illustrates the correlation matrix. Length (L) shows a strong positive correlation with the length-to-diameter ratio (L/D) (0.87), indicating that as length increases, L/D also increases significantly. The correlation between L and thickness (t) (0.11) is weak,

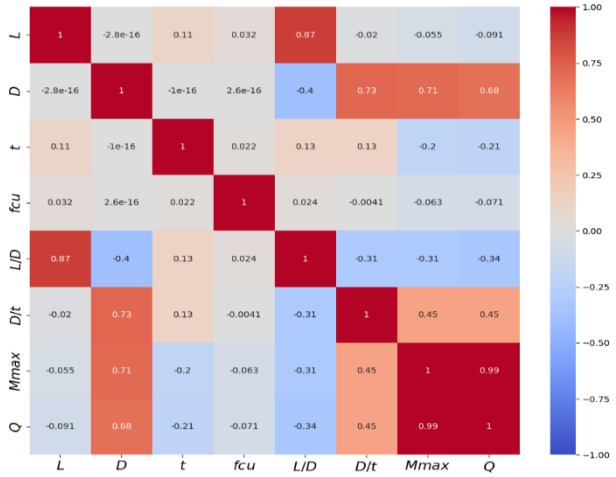

Figure 25:Heatmap correlation matrix

The correlation matrix reveals weak relationships between the thickness of the FRP tube (t) and other parameters: a slight positive correlation with length (L) at 0.11, and a similarly weak positive correlation with both length-to-diameter ratio (L/D) and diameter-to-thickness ratio (D/t) at 0.13. Counterintuitively, thickness exhibits weak negative correlations with maximum moment (Mmax) at -0.2 and shear force (Q) at -0.21, suggesting a potential slight decrease in these performance metrics with increasing thickness, though other factors likely play a more significant role.

The strength of the concrete used in the pile (fcu) doesn't seem to have a strong linear connection with the pile's dimensions or ratios.

While the correlation matrix indicates a moderate negative correlation between the length-to-diameter ratio (L/D) and both shear force (Q) and maximum moment (Mmax) (-0.31 and -0.34, respectively), Figure 8: through Figure 11: demonstrate a different trend. Specifically, these figures show that Mmax and Q increase with increasing L/D up to approximately L/D = 10, after which they slightly decrease and then plateau. This discrepancy suggests that the relationship between suggesting a minor influence of length on thickness. Additionally, L has no significant correlations with other parameters.

The correlation between diameter (D) and the L/D ratio is negative (-0.4), indicating that as the diameter increases, the L/D ratio decreases. This is expected, as D is in the denominator of the L/D ratio. A strong positive relationship is observed between D and the D/t ratio, with a correlation of 0.73. This suggests that an increase in the pile's diameter tends to result in a proportional increase in the diameter-to-thickness (D/t) ratio. The diameter of the FRP tube pile has a substantial positive impact on both its maximum moment capacity and shear force resistance (0.71 and 0.68, respectively). This implies that increasing the pile's diameter is an effective method to enhance its structural performance under bending and shear loads.

L/D and Mmax /Q is likely nonlinear and more accurately represented by the graphical data.

The diameter-to-thickness ratio (D/t) shows a moderate positive correlation with both shear force (Q) and maximum moment (Mmax) at (0.45). Indicating that as D/t increases, Q and Mmax also increases significantly.

5. CONCLUSIONS

After studying the effect of lateral loads on concrete-filled *FRP* piles and examining various parameters such as pile dimensions, the length-to-diameter (*L/D*) ratio, and the diameter-to-thickness (*D/t*) ratio in the soil conditions of East Port Said, as well as analyzing the correlation between the varying parameters and pile capacity, the following results were observed:

- Verification of the present technique of analyzing laterally loaded concrete-filled *FRP* piles embedded in multi-layered soil shows a good agreement with the available interaction diagram in the *ECP* [4], experimental data reported by *Rocca et al.* [28], and the full scale test represented by *Rollins et al.* [29].
- Maximum bending moment and shear force were found to be influenced by the length-to-diameter ratio up to 15, beyond which further increases had no impact as the pile reached its effective length.
- Concrete strength has a negligible impact on the lateral load capacity of the pile, likely due to soil failure occurring before material failure.
- Based on the correlation analysis, pile diameter (*D*) demonstrates a strong positive linear impact on both maximum moment (M_{max}) (0.71) and shear force (*Q*) (0.68). Conversely, the diameter-to-thickness ratio (*D/t*) shows a moderate positive correlation with both shear force (*Q*) and maximum moment (M_{max}) at (0.45). In contrast, concrete compressive strength (f_{cu}) exhibits negligible linear correlations with the other variables examined.
- While the correlation analysis provides valuable insights into linear relationships, it's important to note

that the relationships between L/D and maximum moment (M_{max}) or shear force (Q) are likely nonlinear. Therefore, graphical representations would offer a more accurate depiction of these relationships.

Acknowledgments
This research was self-supported without any type of funding.

Conflicts of Interest
The authors state that there are no conflicts of interest regarding the publication of this research.

6. REFERENCES

[1] A.C.I. Committee (2019). Building code requirements for structural concrete (ACI 318-19) and commentary (ACI 318R-19). *Amesrican Concrete Institute*.

[2] Al-Darraji, F., Sadique, M., Yu, Z., Shubbar, A., & Marolt Čebašek, T. (2025). Performance of Confined Concrete-Filled Aluminum Tube Pile Groups under Combined Loading. Geotechnical and Geological Engineering, **43**(2), 58. https://doi.org/10.1007/s10706-024-03002-0

[3] B. C. I. No, "International building code," 2012.

[4] E.C.P. Committee (2020). Egyptian Code for Design and Construction of Concrete Structures (ECP 203-2020). *Hous. Build. Natl. Res. Cent.*, Cairo, Egypt.

[5] Dhatrak, A. I., Bhadke, S. N., & Thakare, S. W. (2022). Numerical Analysis of load-carrying capacity of fibre-reinforced polymer piles. Ground Characterization and Foundations: Proceedings of Indian Geotechnical Conference 2020 Volume 1, 807–817.

[6] El Gendy, M. Analyzing laterally loaded piles in multi-layered cohesive soils: a hybrid beam on nonlinear Winkler foundation approach with case studies and parametric study. Discov Civ Eng **2**, 77 (2025). https://doi.org/10.1007/s44290-025-00240-w

[7] El Gendy, M. El Gendy, A. (2024). Analysis and design of raft and piled Raft-Program ELPLA. In. Calgary AB, Canada: GEOTEC Software Inc.

[8] El Gendy, M. Formulation of a composed coefficient technique for analyzing large piled raft. *Ain Shams Eng J* **41**(1), 29-56 (2007).

[9] El Gendy, M., El Arabi, I., ELbarbary, A., Hamed, M. Comparative study of structural behavior of *CFRP* tubes and traditional steel for pile and column applications compliance with international codes. Discov Civ Eng **2**, 77 (2025). https://doi.org/10.1007/s44290-025-00244-6

[10] El Gendy, M., El Arabi, I., Kamal, M. Comparative analyses of large diameter bored piles using international codes. *DFI J: J Deep Found Inst* **8**(1), 15-26 (2014). http://dx.doi.org/10.4236/eng.2013.510096

[11] El Gendy, M., El Gendy, O. *Analysis of Piled raft of Burj Khalifa in Dubai by the program ELPLA*. Retrieved from Calgary AB, Canada: GEOTEC Software Inc. (2018).

[12] El Gendy, M., Hanisch, J., Kany, M. Empirical nonlinear analysis of piled raft. *Bautechnik,* **83**(9), 1-32 (2006).

[13] El Gendy, M., Ibrahim, H., El Arabi, I. Analysing Rectangular Pile Using One Dimensional Finite Element. *Geotech Geol Eng* **38**(5), 4617-4635 (2020). https://doi.org/10.1007/s10706-020-01314-5

[14] El Gendy, M., Ibrahim, H., El Arabi, I. COMPOSED COEFFICIENT TECHNIQUE FOR MODELLING BARRETTE GROUPS. *Malays J Civ Eng* **31**(1), 23-33 (2019). https://doi.org/10.11113/mjce.v31n1.510

[15] El Gendy, M., Ibrahim, H., El Arabi, I. Developing the composed coefficient technique for analyzing laterally loaded barrettes. *Innov Infrastruct Solut* **5**(2), 43-43 (2020). https://doi.org/10.1007/s41062-021-00535-8

[16] El Gendy, M., Ibrahim, H., El Arabi, I. The behavior of laterally loaded barrette groups using hybrid flexibility coefficient and finite element technique. *Innov Infrastruct Solut* **6**(3), 170-170 (2021). https://doi.org/10.1007/s41062-020-00294-y

[17] Elkamash, W., Elgendy, M., Salib, R. *et al.* Studying of Shear Walls with Piled Raft over Soft Soil against Seismic Loads. *PSERJ* **18**(1), 144-155 (2014). https://dx.doi.org/10.21608/pserj.2014.46816

[18] Ghatass, H., El Arabi, I., El Gendy, M. Analyzing Barrettes as Large-Section Supports by CCT. *PSERJ* **20**(2), 27-39 (2016). https://dx.doi.org/10.21608/pserj.2016.33578

[19] Ibrahim, F., El Gendy, M., Salib, R. *et al.* Nonlinear analysis of piled raft with 3D-space structure. *PSERJ* **13**(2), 1-21 (2009).

[20] Kim, S.-H. (2024). Characterization of Flexural Behavior of Hybrid Concrete-Filled Fiber-Reinforced Plastic Piles. Materials, **17**(5), 1072. https://doi.org/10.3390/ma17051072

[21] Kim, S.-H., Joo, H.-J., & Choi, W. (2024). Structural Behavior of High Durability FRP Helical Screw Piles Installed in Reclaimed Saline Land. Polymers, **16**(12), 1733. https://doi.org/10.3390/polym16121733

[22] Lee, S. W., Choi, S., Kim, B.-S., Kim, Y.-J., & Park, S.-Y. (2002). Structural characteristics of concrete-filled glass fiber reinforced composite piles. Proc. Third International Conference on Composites in Infrastructure, San Francisco, California, USA.

[23] Malik, N., Chen, W.-B., Wu, P.-C., Chen, Z.-J., & Yin, J.-H. (2025). Axial and Circumferential Behavior of Rock-Socketed FRP-SSC Composite Piles Monitored by Distributed Optical Fiber Sensors. Journal of Geotechnical and Geoenvironmental Engineering, 151(4), 4025006. https://doi.org/10.1061/JGGEFK.GTENG-12367

[24] Mohamedien, M., El Gendy, M., El Araby, I. *et al.* Reducing Settlement Using Piled Raft for Neighboring Foundations in Port-Said. *PSERJ* **17**(2), 136-146 (2013). https://dx.doi.org/10.21608/pserj.2013.50588

[25] Otoom, O. F., Lokuge, W., Karunasena, W., Manalo, A. C., Ozbakkaloglu, T., & Thambiratnam, D. (2021). Experimental and numerical evaluation of the compression behaviour of GFRP-wrapped infill materials. Case Studies in Construction Materials, 15, e00654.

[26] Pando, M., Lesko, J., Fam, A., & Rizkalla, S. (2002). Durability of concrete-filled tubular FRP piles. The 3rd Int. Conf. on Composites in Infrastructure, ICCI, 2, 10–12.

[27] Reese, L., Wang, S., Isenhower, W. *et al.* Computer Program *LPILE* Plus. Ensoft, Austin, TX. (2022).

[28] Rocca, S., Galati, N., Nanni, A. Interaction diagram methodology for design of FRP-confined reinforced concrete columns. *Constr Build Mater* **23**(4), 1508-1520 (2009). https://doi.org/10.1016/j.conbuildmat.2008.06.010

[29] Rollins, K., Peterson, K., Weaver, T. Lateral Load Behavior of Full-Scale Pile Group in Clay. *Journal of Geotechnical and Geoenvironmental Engineering* **124**(6), 468-478 (1998). https://doi.org/10.1061/(ASCE)1090-0241(1998)124:6(468)

[30] Russo, G. Numerical analysis of piled rafts. *Int J Numer Anal Methods Geomech* **22**(6), 477-493 (1998). https://doi.org/10.1002/(SICI)1096-

9853(199806)22:6%3C477::AID-NAG931%3E3.0.CO;2-H
[31] *RSPile*. A lateral pile analysis software program, Toronto, Canada, (2024).
[32] SNI 8460-2017 Indonesian Geotechnical Designing Guidelines.
[33] *SPColumn*. Design and investigation of reinforced concrete column sections, USA, (2024).
[34] Zhang, S., Miao, K., Wei, Y., Xu, X., Luo, B., & Shi, W. (2023). Experimental and Theoretical Study of Concrete-Filled Steel Tube Columns Strengthened by FRP/Steel Strips Under Axial Compression. International Journal of Concrete Structures and Materials, **17**(1), 1–22.
[35] Yong, Y (2024). A lateral pile analysis software program PyPile. Edmonton, Alberta, Canada: Yong Technology Inc.